EPR of Eu^{2+} in $Pb_{1-x}Eu_xSe$ layer and in $Pb_{1-x}Eu_xSe/PbSe$ superlattice grown by molecular-beam epitaxy on BaF_2 substrates

X. Gratens, A. B. Arauzo,* G. Breton, S. Charar, and M. Averous
Groupe d'Etude des Semiconducteurs UMR 5650, Université Montpellier II, Place Eugène Bataillon, 34095 Montpellier Cedex 5, France

S. Isber
Department of Physics, Concordia University, 1455 de Maisonneuve Boulevard West, Montreal, Quebec, Canada H3G 1M8
(Received 13 January 1998)

Electron paramagnetic resonance (EPR) experiments are performed at room and liquid helium temperature on layers $Pb_{1-x}Eu_xSe$ and on the superlattice $PbSe/Pb_{1-x}Eu_xSe$, grown by molecular beam epitaxy. EPR measurements show unambiguously that Eu^{2+} ions replace the Pb^{2+} ions and that the crystal field is associated with an octahedron of Se^{2-} ions in the $Pb_{1-x}Eu_xSe$ epitaxial layer. The data were fitted with the classical cubic spin Hamiltonian. The crystal field coefficients are $b_4=267.4$ MHz and $b_6=-3.4$ MHz. Low-temperature experiments do not reveal the existence of strain in the epitaxial layers and in the superlattices. The effect of the europium concentration on the EPR spectrum can be characterized by (i) the vanishing of the fine structure, (ii) the appearance of a strong central transition, (iii) the broadening of the transition due to the Eu^{2+} nearest-neighbor dipolar and exchange interactions.
[S0163-1829(98)03126-9]

I. INTRODUCTION

Electron paramagnetic resonance (EPR) measurements on low concentration divalent europium ions in semiconductors such as the lead chalcogenides[1–3] give information about the local symmetry and the crystal field associated with the rare-earth site in rock salt structures. The EPR spectra of isolated Eu^{2+} has been extensively studied in a wide range of environments. They are well known in the case where some Eu^{2+} ions substitute for Pb^{2+} ions in the bulk diamagnetic lead chalcogenides PbSe (Refs. 1 and 2), PbS (Ref. 3), and PbTe.[4] Let us recall that the EPR spectrum of an isolated Eu^{2+} ion in a IV-VI host with a rock salt structure is strongly dependent on the angle between the external applied magnetic field and the crystal axis. This anisotropy is the result of the splitting of the Eu^{2+} electronic levels by the host crystal field. For the orientation for which the fine structure splitting is largest ($\mathbf{H}\|[001]$), the spectrum consists of seven fine lines roughly symmetrical about the central transition. The paramagnetic resonance characteristics of Eu^{2+} in PbSe are therefore used to investigate the crystallographic quality and the microscopic environment in the case of the $Pb_{1-x}Eu_xSe$ crystal growth by molecular-beam epitaxy (MBE).

In this paper we report and discuss the EPR results on a series of $Pb_{1-x}Eu_xSe$ epitaxial layers (EL's) and on $Pb_{1-x}Eu_xSe/PbSe$ multiquantum well (MQW) heterostructures. The EPR study includes comparison with bulk crystalline results. All EL's and MQW's were grown by reflection high-energy electron diffraction (RHEED) controlled molecular beam epitaxy, using a 2300 Riber MBE system and effusion cells for PbSe and Eu, on freshly cleaved (111) face of commercial BaF_2 substrates, which are used for PbSe growth because of the nearly lattice constant and thermal expansion coefficient. The europium concentration ($x=0.01$, 0.03, 0.04, 0.05, and 0.2) in the single EL was determined from microprobe measurements. A Bruker *X*-band (9.54 GHz) spectrometer equipped with an Oxford Instrument helium gas flow and a goniometer for precise sample orientation with respect to the applied magnetic field was used for EPR measurements performed at 300 and 4.2 K. The (111) faces of BaF_2 substrate were used to orient the EL in the cavity.

II. ISOLATED Eu^{2+} IONS IN PbSe SINGLE EPITAXIAL LAYERS

A. Spin Hamiltonian

The EPR line positions of the isolated Eu^{2+} ions were fitted to the classical spin Hamiltonian, which describes the electronic states of the ground state[8] $S_{7/2}$, in a cubic crystal field:[5,6]

$$\mathcal{H}=g\mu_B\mathbf{H}\cdot\mathbf{S}+\frac{b_4}{60}[O_4^0+5O_4^4]+\frac{b_6}{1260}[O_6^0-21O_6^4]. \tag{1}$$

In Eq. (1) the first term describes the Zeeman interaction of the Eu^{2+} ion with the external magnetic field $\mathbf{H}$, g is the Landé factor, μ_B is the Bohr magneton, and S is the spin angular momentum. The second and the last terms describe the interaction between the S-state ion and the crystal field. O_4^m and O_6^m ($m=0,4$) are the fourth and the sixth degree cubic operators as defined by Abragam and Bleaney.[5] b_4 and b_6 are the crystal field coefficients. At zero field, the S state splits into two doublets Γ_6, Γ_7, and one quadruplet Γ_8, with the respective energies $E(\Gamma_6)=14b_4-20b_6$, $E(\Gamma_7)=-18b_4-12b_6$, and $E(\Gamma_8)=2b_4+16b_6$. The overall splitting is given by $\Delta=E(\Gamma_7)-E(\Gamma_6)=-32b_4+8b_6$.

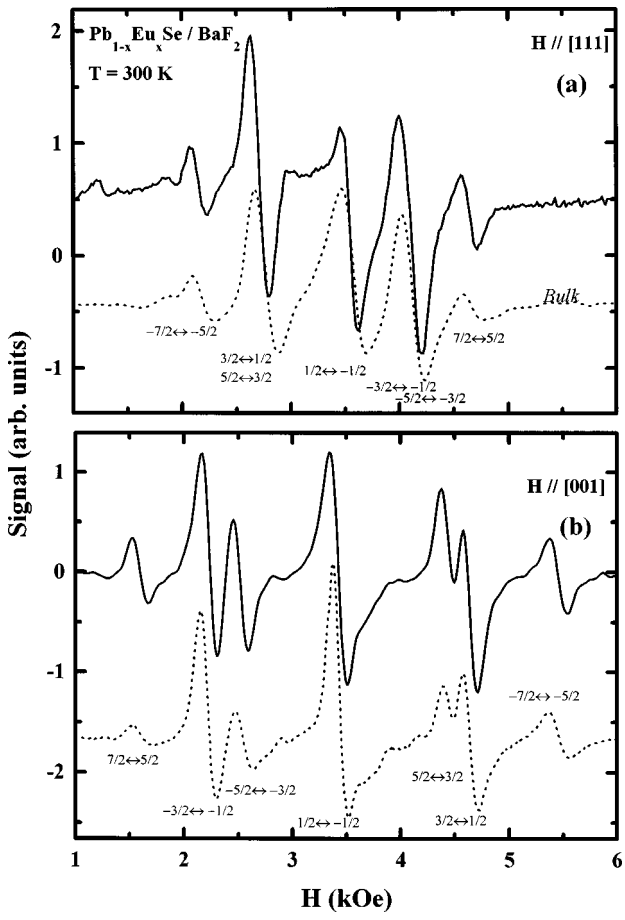

FIG. 1. *X*-band first derivative absorption EPR spectra of the Eu^{2+} in $Pb_{1-x}Eu_xSe/BaF_2$ layer growth by MBE for $\mathbf{H}\|[111]$ (a) and $\mathbf{H}\|[001]$ (b) at 300 K. The dotted line represent the EPR spectra of bulk sample. Asymmetry of the transition about the central absorption is better shown for $\mathbf{H}\|[111]$.

B. EPR spectra

The EPR spectra of $Pb_{1-x}Eu_xSe$ single EL were recorded at 300 and 4.2 K for different orientation of the external magnetic field **H** in the (011) plane. Figures 1(a) and 1(b) show derivative EPR spectra of the $Pb_{1-x}Eu_xSe$ ($x=0.01$) layer at 300 K and for $\mathbf{H}\|[111]$ and $\mathbf{H}\|[001]$. Typical Eu^{2+} spectra in the PbSe bulk sample for the two different directions are exhibited as a dotted line in Fig. 1. For $\mathbf{H}\|[001]$ the EPR spectra is composed of seven allowed transitions $M\leftrightarrow M-1$ (where $M=\frac{7}{2}, \frac{5}{2}, \frac{3}{2}, \frac{1}{2}, -\frac{1}{2}, -\frac{3}{2}, -\frac{5}{2}, -\frac{7}{2}$ is the electronic magnetic quantum number) while the EPR spectra for $\mathbf{H}\|[111]$ is composed of only five EPR lines. As can be seen in Fig. 1, the spectra are not symmetrical about the central line. For $\mathbf{H}\|[001]$ the separation between the $-\frac{5}{2}\leftrightarrow -\frac{3}{2}$ and $-\frac{3}{2}\leftrightarrow -\frac{1}{2}$ transitions is larger than the $(+\frac{5}{2}\leftrightarrow +\frac{3}{2})$ and $(+\frac{3}{2}\leftrightarrow +\frac{1}{2})$ ones. For $\mathbf{H}\|[111]$ the asymmetry is better shown comparing the separation of the two extreme lines $-\frac{7}{2}\leftrightarrow -\frac{5}{2}$ and $\frac{7}{2}\leftrightarrow \frac{5}{2}$ from the central $-\frac{1}{2}\leftrightarrow \frac{1}{2}$ line.

It is seen in Fig. 1 that the positions of the EPR lines of the Eu^{2+} substituting for the Pb^{2+} ions in the bulk sample grown by the Bridgman method and the EL grown by MBE are found to be practically the same within the experimental error. Meanwhile, the shapes of the EPR lines are different. At 300 K, the Dysonian line shape due to the metal-like behavior is not observed in the case of the EL. Electrical transport measurements have shown that the EL ($x=0.01$) was a *p*-type semiconductor with a carrier concentration $p=3.16\times10^{17}$ cm^{-3} and resistivity $\rho=0.0731\ \Omega$ cm which is close to the value for bulk sample. For the EL with a small thickness (2 μm) compared to the penetration depth [$\delta=(\rho/\pi\mu\nu)^{1/2}=0.14$ mm for $\rho=0.0731\ \Omega$ cm and $\nu=9.54$ GHz], the energy absorption is not dependent on the electron diffusion. Thus the skin effect leaves the observed Gaussian shape of the EPR line unchanged.

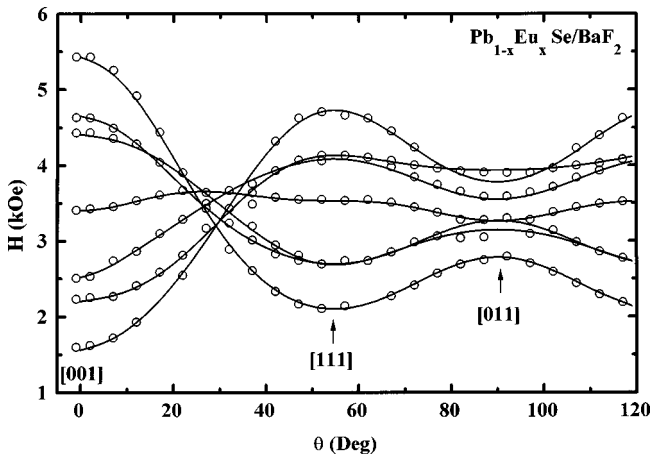

FIG. 2. Angular variation of the resonance field for the seven allowed transitions of the Eu^{2+} fine structure at 300 K. The external magnetic field rotates in the (011) plane of the layer. The full circles represent the observed transitions and the lines represent the calculated resonance by the diagonalization of the spin Hamiltonian matrix using the parameters $g=1.975$, $b_4=267.4$ MHz, and $b_6=-3.4$ MHz.

At 300 K and for $\mathbf{H}\|[001]$ the experimental intensities of the seven allowed transitions agree with the theoretical values calculated from the spin Hamiltonian of the isolated ions $[S(S+1)-M(M-1)]$. For instance the experimental intensity ratio of $+\frac{1}{2}\leftrightarrow -\frac{1}{2}$ to the $-\frac{7}{2}\leftrightarrow -\frac{5}{2}$ is 16:5.5 for the layer instead of the theoretical 16:7. For bulk sample, we have found 16:4.5. The distribution of $E(\Gamma_6)$ and $E(\Gamma_7)$ values for Eu^{2+} observed in the case of the bulk samples[1,2] is not present in the EL.

Figure 2 exhibits the measured angular dependence of the magnetic field for resonance corresponding to the seven allowed transitions of isolated Eu^{2+} ions in the $Pb_{1-x}Eu_xSe$ EL ($x=0.01$) when the magnetic field direction rotates in the (011) plane. The position of the EPR lines are determined without Dyson analysis[7,8] of the line shape. In first approximation the angular variation of the seven allowed transitions field follows approximately the relation

$$1-5\sin^2\theta+(15/4)\sin^4\theta, \tag{2}$$

in which θ is the angle between the magnetic field and the [001] crystal axis.

The examined single epilayer revealed an intense single line spectrum for θ close to 30°. In Fig. 2, the solid lines represent the best fit of the experimental data to the theoretical fields for resonance determined from the exact diagonalization of the (8×8) matrix. The values of the crystal field coefficients are $b_4=267.4$ MHz and $b_6=-3.4$ MHz at 300 K, while the values for bulk sample were found to be b_4

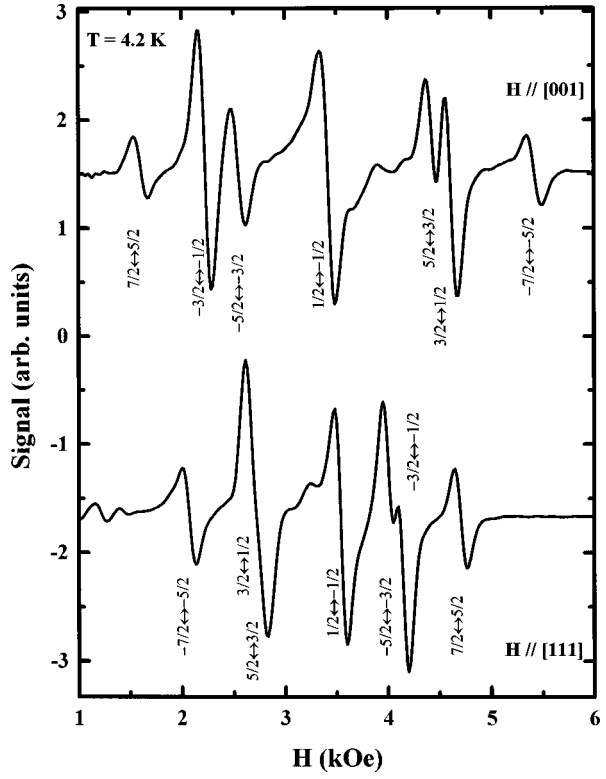

FIG. 3. *X*-band first derivative absorption EPR spectra of the Eu^{2+} in $Pb_{1-x}Eu_xSe/BaF_2$ layer growth by MBE, for $\mathbf{H}\|[111]$ and $\mathbf{H}\|[001]$ at 4.2 K. The spectrum for $\mathbf{H}\|[111]$ is better resolved.

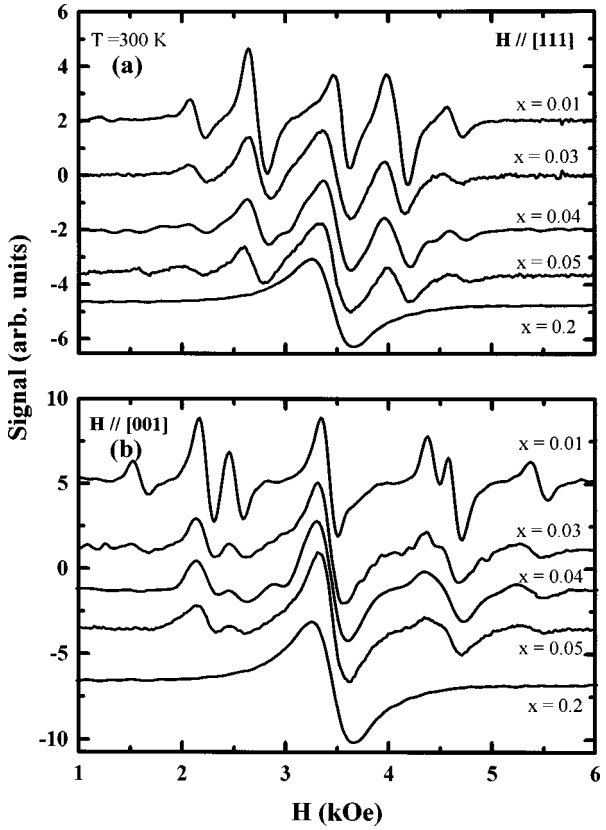

FIG. 4. Different Eu^{2+} concentration $Pb_{1-x}Eu_xSe/BaF_2$ EPR spectra performed at 300 K for $\mathbf{H}\|[111]$ and $\mathbf{H}\|[001]$. The fine structure vanishes with the increase of the composition. For the high composition, the spectra consist of a large central position.

$=269$ MHz and $b_6=-5.8$ MHz at 300 K. We think that the small discrepancy is due to the Dysonian line shape analysis used for the bulk sample. The EPR linewidths corresponding to the transitions $M\leftrightarrow M-1$ and $-M\leftrightarrow-(M-1)$ for $\mathbf{H}\|[001]$ were found to be the same as those for $\mathbf{H}\|[111]$.

Figure 3 shows the EPR spectrum measured at 4.2 K, the fine structure of Eu^{2+} in the EL is typical of a cubic crystal field splitting. The estimated value of the crystal field coefficients are found to be the same as those at 300 K. The EPR lines are not affected by the skin effect ($\rho=0.0014\ \Omega$ cm, $\delta=19\ \mu$m). For $\mathbf{H}\|[111]$ the fine structure is better resolved at 4.2 K than at room temperature. This is due to the dependence on temperature of the EPR linewidths. The peak to peak average width of the EPR lines shape at 300 K is about 140 G, decreasing to 110 G at 4.2 K. Below about 20 K, the $-\frac{5}{2}\leftrightarrow-\frac{3}{2}$, $-\frac{3}{2}\leftrightarrow-\frac{1}{2}$ pair of transition becomes resolved while the $+\frac{5}{2}\leftrightarrow+\frac{3}{2}$, $+\frac{3}{2}\leftrightarrow+\frac{1}{2}$ pair of transition is not resolved. Thus the asymmetry of the EPR spectrum due to the effect of the cubic crystal field is clearly shown and it can be accounted for only if b_4 and b_6 have opposite signs.

The absolute signs of b_4 and b_6 were confirmed from measurements of the relative intensities of the $-\frac{7}{2}\leftrightarrow-\frac{5}{2}$, $+\frac{7}{2}\leftrightarrow\frac{5}{2}$ transition at 4.2 and 300 K. The increase in intensity of the high-field line for $\mathbf{H}\|[001]$ and the low-field line for $\mathbf{H}\|[111]$ gives rise to the Γ_6 doublet as a fundamental state at zero field.

In the 4.2–300 K temperature range, the estimated Landé factor g values were found to be independent of temperature $g=1.975\pm0.002$. The difference between free electron spin and experimental values of Landé factor can be explained by the influence of the excited states on the ground state. The coefficient α, which represents the admixture between the $^8S_{7/2}$ and $^6P_{7/2}$ states has been estimated as 0.3 from the expression of Lacroix[9]

$$g=(1-\alpha^2)^2 g_s+\alpha^2 g_p\,, \tag{3}$$

where g_s and g_p are the g values for $^8S_{7/2}$ and $^6P_{7/2}$ states. The value of α is very close to the values estimated in the case of $Pb_{1-x}Eu_xSe$ (Refs. 1 and 2) ($\alpha=0.25$) and $Pb_{1-x}Eu_xS$ (Ref. 3) ($\alpha=0.3$) bulk samples. It is seen in Figs. 1(a) and 3 that in addition to the seven intense allowed fine structure lines there appeared three forbidden ($\Delta M=\pm2$) transitions at low field which are attributed to the transitions $\frac{7}{2}\leftrightarrow\frac{3}{2}$ ($H=1945$ G), $-\frac{7}{2}\leftrightarrow-\frac{3}{2}$ ($H=1273$ G), and $-\frac{1}{2}\leftrightarrow\frac{3}{2}$ ($H=1479$ G).

III. EFFECT OF THE Eu^{2+} CONCENTRATION

Figures 4(a) and 4(b) show the dependence of the EPR spectrum on x, for the single EL's with concentration $x=0.01-0.20$. The thickness of the EL's varied from 1.5 to 2 μm. For $\mathbf{H}\|[111]$ and $\mathbf{H}\|[001]$ the effect of the incorporation of europium in the PbSe lattice on the EPR lines of the allowed transitions is clearly shown. First, the EPR linewidths increased with increasing Eu^{2+} concentration (Fig. 5). Such behavior is attributed to the Eu^{2+}-Eu^{2+} dipolar and exchange interactions.[10,11]

Second, the fine structure of Eu^{2+} ions vanished with increasing x. The positions of the seven allowed transitions

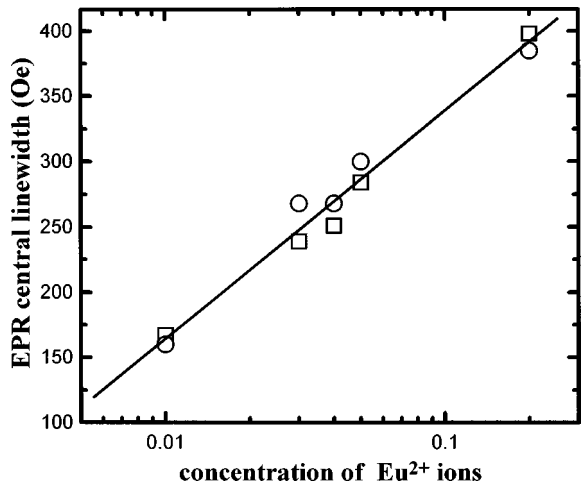

FIG. 5. Linear variation of the full half line width for the $\frac{1}{2}\leftrightarrow -\frac{1}{2}$ transition versus log(x), for the $\mathbf{H}\|[001]$ (circle) and for $\mathbf{H}\|[111]$ (square).

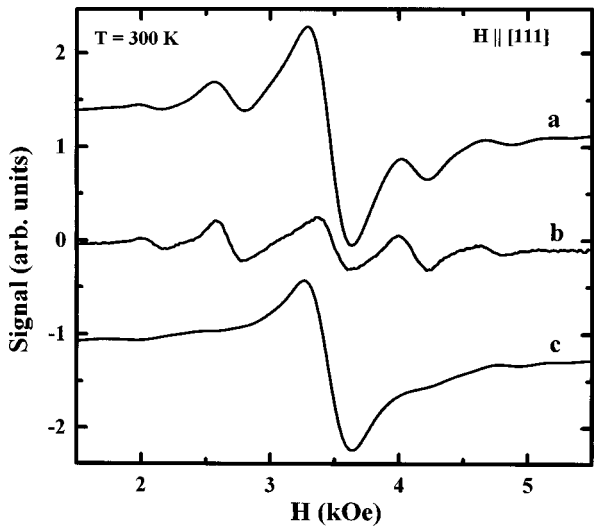

FIG. 6. (a) EPR spectrum at 300 K of a $Pb_{1-x}Eu_xSe/PbSe$ MQW for the $\mathbf{H}\|[111]$. (b) EPR spectrum at 300 K of a single $Pb_{1-x}Eu_xSe$ layer ($x=0.04$). (c) Strong and broad EPR lines determined by subtraction of the signals a and c. This line is attributed to the Eu^{2+} cluster resonance.

are found to remain the same but the ratio of the experimental intensity of the $\frac{1}{2}\leftrightarrow -\frac{1}{2}$ transition to the other $M\leftrightarrow M-1$ lines increased with increasing value of x from 0.01 to 0.05. For $x=0.2$ EL, the EPR signal is not anisotropic and the spectrum consists of an isotropic central line.

To summarize, the increase in the Eu^{2+} concentration results in a gradual disappearance of the typical fine structure due to the isolated ions and in an increase in the intensity of the central line. There are two possibilities to explain the dependence of the EPR results as a function of x. First, the incorporation of europium in the PbSe lattice can affect the structural quality of the EL. Disorder in the atomic arrangement in the $Pb_{1-x}Eu_xSe$ lattice or mosaiciness of the EL affect the EPR lines which depend on the orientation of the crystal axis.

Secondly, the changes in the the EPR spectrum of the EL with the Eu^{2+} ions concentration can be due to cluster resonance. The statistics of the clusters for a crystal with rock salt structure predict a decrease of the number of the isolated ions with increasing x. In the concentration range $x=0.01-0.05$ the number of single ion clusters exceeds the number of the other cluster types. For the high concentration of europium, the probability to find single ion clusters is zero, and the EPR signal cannot be treated using the spin Hamiltonian of the isolated ions. The following arguments indicate that the second possibility is more likely. First, the full width at half maximum (FWHM), obtained from x-ray diffraction patterns is found to be practically the same (250 arc sec) for the sample with $x=0.01$, 0.03, 0.04, and 0.05. Secondly, microprobe analysis has revealed that the substitution of Pb^{2+} ions by Eu^{2+} is real and that the distribution of the Eu^{2+} ions is random. In addition, magnetization measurements[12] performed on bulk samples have shown that the distribution of Eu^{2+} ions is homogeneous for $x=1.3$, 3, and 4 %.

IV. $Pb_{1-x}Eu_xSe/PbSe$ MULTIQUANTUM WELLS

Five and a fifty $Pb_{1-x}Eu_xSe/PbSe$ MQW's were grown on (111) BaF_2 substrates. The thickness of the individual layer in the two heterostructures is 200 Å. The five MQW's were grown using a $Pb_{1-x}Eu_xSe$ buffer layer (1.5 μm) while the superlattice was grown on a PbSe relaxed buffer layer (1.5 μm). The EPR spectrum of five MQW heterostructures is shown in Fig. 6(a). The observed behavior of the EPR linewidths as a function of x for the single EL's is used to obtain the value $x=0.09$ for the Eu^{2+} concentration in this heterostructure. The shape of the EPR spectrum looks similar to the shape of the EPR line observed for $Pb_{1-x}Eu_xTe/PbTe$ MQW heterostructures grown by hot wall epitaxy.[13] The spectrum is due to the isolated Eu^{2+} ions [Fig. 6(b)], superimposed on a large and isotropic central line [Fig. 6(c)]. For the $Pb_{1-x}Eu_xTe/PbTe$ MQW heterostructure, the authors have attributed the additional EPR line to Eu^{2+} dispersed into the PbTe layers[13] and to a inhomogeneous distribution of europium in the PbTe lattice. Magnetization measurements performed at low temperature on $Pb_{1-x}Eu_xTe$ (Ref. 14) bulk samples have shown that the randominess of the distribution of Eu^{2+} over the cation sites is perfect. As we have seen in the case of the europium doped EL, the concentration x influences the EPR spectrum shape, thus we think that a study of the EPR spectrum change with x must be performed on a single $Pb_{1-x}Eu_xTe$ layer before attributing it to the existence of defects in the crystal.

The 50 period $Pb_{1-x}Eu_xSe/PbSe$ superlattice structure was confirmed by the x-ray diffraction pattern obtained around (444) reflections. Because of the low europium concentration and of the thickness of the individual layer, we assume that the layers are fully relaxed. The EPR spectrum of this $Pb_{1-x}Eu_xSe/PbSe$ MQW heterostructure for $\mathbf{H}\|[111]$ and $\mathbf{H}\|[001]$ and for 4.2 K (Fig. 7) can be interpreted using the spin Hamiltonian of the isolated ions and the parameters determined in the case of the single EL. We found $x=0.017$ (Fig. 4) for the concentration of Eu^{2+} ions in the $Pb_{1-x}Eu_xSe$ layers of the superlattices.

The strain effect on the EPR spectrum, reported in the case of Mn^{2+} in ZnTe/MnTe (Ref. 15) is not present on the spectrum at 4.2 K. Because of the small content of Eu, the

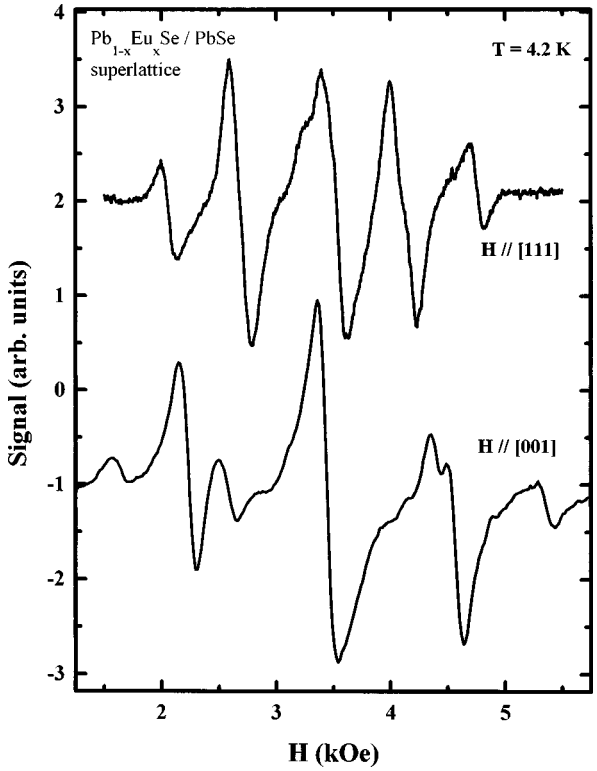

FIG. 7. *X*-band first derivative absorption EPR spectra of the Eu^{2+} in the $Pb_{1-x}Eu_xSe$/PbSe superlattice grown on a thick PbSe buffer layer by MBE for $\mathbf{H}\|[111]$ and $\mathbf{H}\|[001]$ at 4.2 K. The experimental EPR result (anisotropy, fine structure of the isolated ions) are very well interpreted using the Eu^{2+} spin Hamiltonian and the crystal field coefficients of the PbSe lattice. No strain induced by the lattice mismatch is observed.

lattice mismatch between PbSe and $Pb_{1-x}Eu_xSe$ is estimated to be only 0.1%, therefore, the layers are strain relaxed.

V. SUMMARY AND CONCLUSION

The EPR measurements performed on the $Pb_{1-x}Eu_xSe$ EL and on the $Pb_{1-x}Eu_xSe$/PbSe superlattice show crystalline perfection for low europium concentrations ($x<5\%$) necessary for sensor narrow-gap materials. The two fine structures, for $\mathbf{H}\|[111]$ and $\mathbf{H}\|[001]$, and the angular variation of the resonant field in the (011) planes are interpreted using the cubic spin Hamiltonian and the crystal field coefficients are found to be close to the values obtained from the bulk sample EPR measurements. The asymmetry observed is attributed to the crystal field coefficients as in the case of Gd^{3+} diluted in Bi_2Se_3.[16]

The EPR lines are not Dysonians contrary to the EPR lines of the bulk sample. The g factor is found to be isotropic for all the epilayers ($g=1.975$). The EPR spectrum of Eu^{2+} in $Pb_{1-x}Eu_xSe$ is very sensitive to the orientation of the applied magnetic field, the temperature, and the number of the isolated ions in the host lattice. The changes in the EPR spectrum observed with the concentration are attributed to the effect of the europium cluster resonance and the vanishing of the fine structure due to the isolated ions is associated with the decrease of the probability finding isolated ions in the lattice with increasing x.

EPR measurements performed on superlattices show that the crystal field is cubic. The EPR spectrum agree with the crystal field coefficient of a single EL.

ACKNOWLEDGMENTS

The authors would like to thank Y. Shapira (Tuffs University, Boston) for helpful discussions and C. Merlet (Montpellier II) for microprobe analysis. This work was supported by the Centre National de la Recherche Scientifique (France).

*Present address: Instituto de Ciencio de Materiales de Aragon, UZ-CSIC, Pza. S. Francisco s/n 50009 Zaragoza, Spain.

[1] S. Isber, S. Charar, C. Fau, V. Mathet, M. Averous, and Z. Golacki, Phys. Rev. B **52**, 1678 (1995).
[2] S. K. Misra, Y. Chang, V. Petkov, S. Isber, S. Charar, C. Fau, M. Averous, and Z. Golacki, J. Phys.: Condens. Matter **7**, 9897 (1995).
[3] S. Isber, S. K. Misra, S. Charar, X. Gratens, M. Averous, and Z. Golacki, Phys. Rev. B **56**, 8199 (1997).
[4] G. B. Bacskay, P. J. Fensham, I. M. Ritchie, and R. N. Ruff, J. Phys. Chem. Solids **30**, 713 (1969).
[5] A. Abragam and B. Bleaney, *Electron Paramagnetic Resonance of Transition Ions* (Clarendon, Oxford, 1972), Vol. 1.
[6] K. R. Lea, M. J. M. Leask, and W. P. Wolf, J. Phys. Chem. Solids **23**, 1381 (1962).
[7] F. J. Dyson, Phys. Rev. **98**, 349 (1955).
[8] M. Peter, D. Shaltiel, and J. H. Wernick, Phys. Rev. **126**, 139 (1962).
[9] R. Lacroix, Helv. Phys. Acta **30**, 374 (1957).
[10] S. K. Misra and S. I. Andronenko, Phys. Rev. B **53**, 11 631 (1996).
[11] S. Isber, M. Averous, Y. Shapira, V. Bindilatti, A. N. Anisimo, N. F. Oliveira, Jr., V. M. Orera, and M. Demianiuk, Phys. Rev. B **51**, 15 211 (1995).
[12] V. Bindilatti, N. F. Oliveira, Y. Shapira, Jr., G. H. McCabe, M. T. Liu, S. Isber, S. Charar, M. Averous, E. J. McNiff, Jr., and Z. Golaki, Phys. Rev. B **53**, 5472 (1996).
[13] T. Nakamura, A. Ishida, and H. Fujiyasu, Thin Solid Films **161**, 149 (1988).
[14] E. T. Haar, V. Bindilatti, N. F. Oliveira, Jr., G. H. McCabe, Y. Shapira, Z. Golacki, S. Charar, M. Averous, and E. J. McNiff, Jr., Phys. Rev. B **56**, 8912 (1996).
[15] M. Qazzaz, G. Yang, S. H. Xin, L. Montes, H. Luo, and J. K. Furdyna, Solid State Commun. **96**, 405 (1995).
[16] X. Gratens, S. Isber, S. Charar, C. Fau, M. Averous, S. K. Misra, Z. Golacki, M. Ferhat, and J. C. Tedenac, Phys. Rev. B **55**, 8075 (1997).